ASTM INTERNATIONAL

Journal of Testing and Evaluation

Philip Egberts,[1] Nicholas Simin,[2] Calvin Wong,[2] Jan Czibor,[2] Curtis Ewanchuk,[2] and Simon Park[2]

DOI: 10.1520/JTE20170468

A Novel Tribometer Designed to Evaluate Geological Sliding Contacts Lubricated by Drilling Muds

Journal of Testing and Evaluation

doi:10.1520/JTE20170468 available online at www.astm.org

Philip Egberts,[1] Nicholas Simin,[2] Calvin Wong,[2] Jan Czibor,[2] Curtis Ewanchuk,[2] and Simon Park[2]

A Novel Tribometer Designed to Evaluate Geological Sliding Contacts Lubricated by Drilling Muds

Reference

Egberts, P., Simin, N., Wong, C., Czibor, J., Ewanchuk, C., and Park, S., "A Novel Tribometer Designed to Evaluate Geological Sliding Contacts Lubricated by Drilling Muds," *Journal of Testing and Evaluation* https://doi.org/10.1520/JTE20170468.
ISSN 0090-3973

ABSTRACT

Great interest in improving lubricity, or reducing friction, of drilling muds used for horizontal oil well drilling is motivated by increasing the horizontal reach that can be attained by a single drilling site. However, there are a limited number of commercially available devices that can be used to evaluate novel drilling mud solutions under sliding conditions that accurately replicate those encountered in the field, and those that are available are often prohibitively expensive. Here, the design of a low-cost lubricity meter, or tribometer, is documented. The purpose-built tribometer is capable of varying rotating speeds, applied normal loads, temperature, and counter surface materials. In particular, the counter surface of the tribometer can be either a steel surface, as is often used in the industrial lubricity meters available in corporate laboratories, or a geological core specimen taken from the drill site. The novel instrument was then used to evaluate four commercially available water-based drilling fluid lubricant additives, dissolved in distilled water, for both a steel-on-steel contact and a steel-on-rock contact. The steel-on-steel contact shows that the tribometer replicates the results of tests typically conducted in drilling fluid labs, thus verifying the performance of the newly developed tribometer. Additional results show that the friction and performance of the lubricant depend significantly on the materials used: steel-on-steel contacts show much lower friction than steel-on-sandstone contact. Finally, a weak

Manuscript received August 9, 2017; accepted for publication February 9, 2018; published online August 10, 2018.

[1] Department of Mechanical and Manufacturing Engineering, Schulich School of Engineering, University of Calgary, 40 Research Place NW, Calgary, AB T2L 1Y6, Canada (Corresponding author), e-mail: philip.egberts@ucalgary.ca, https://orcid.org/0000-0002-3353-4493

[2] Department of Mechanical and Manufacturing Engineering, Schulich School of Engineering, University of Calgary, 40 Research Place NW, Calgary, AB T2L 1Y6, Canada

dependence on the applied load is shown for a number of lubricant additives examined.

Keywords

oil production, friction test methods, water-based lubrication, steel, sandstone

Introduction

One of the major advances in oil and gas resource extraction as well as pipeline routing has been subsurface horizontal oil well drilling. This technology has allowed for the exploitation of large oil and gas reservoirs using a reduced number of well sites as well as the routing of pipelines beneath geological barriers [1,2]. Currently, a limit in the reach, or the horizontal distance that can be drilled from the oil platform, is approximately 11 km [1], having increased from 8 km [2] over the past 20 years. A desire to increase the reach limit in horizontal well drilling allows for larger spacing and fewer drill sites to be constructed to extract oil from a single formation [1]. The impact of increased reach limits for horizontal well drilling has been particularly important for both industry and environmental reasons: lower costs and capital investments can be realized with longer reach distances, as well as less damage of the land on the surface of the earth as oil fields are often located in environmentally sensitive regions of the country. However, friction between the drill string (steel casings) and geological formations (rocks) has been one of limiting factors for reaching deeper and longer. To overcome this challenge, several researchers and companies have been developing improved lubricants (also known as muds) to reduce friction.

The use of water-based fluids is more desirable in comparison with oil-based fluids, as they are typically less damaging to the environment [3–5]. These water-based drilling muds typically contain a number of additives, including surfactants, thickening agents (viscosifiers), and corrosion inhibitors. In general, the performance of water-based muds is often dictated by the types of additives and their relative concentrations within the drilling mud. As there is no predictive theory that can be used to identify the optimal formulation of these additives within a water-based mud, each must be individually assessed experimentally to identify any improvements in the lubricating properties of the mud in reducing the coefficient of friction between the steel drill string and the steel casing or geological formation.

To achieve the goal of an overall unlocking of greater horizontal extents that can be reached in horizontal well drilling operations, an examination of the friction coefficient that is measured both in a steel-on-steel contact and a steel-on-geological formation contact in the presence of a water-based drilling mud is required. Despite the material systems required for an accurate assessment of the performance of drilling mud, most tribometers used in the industry have been designed only to evaluate a drilling mud for a steel-on-steel sliding contact rather than the multitude of material systems that would be encountered on a real-world drilling site [6]. This limitation in the current design of commercially available tribometers thus hinders the development of improved drilling muds, as laboratory scale testing does not provide realistic results.

Additionally, identification of lubrication mechanisms can be extremely important in determining or predicting those additives that would be most effective in novel drilling muds. Identification of lubrication mechanisms for fluid-lubricated contacts is most often realized through the generation of a Stribeck curve [7,8]. In this type of analysis, the

combined influence of the applied pressures between sliding contacts, the viscosity of the fluid, and the sliding speed between the contacts becomes relevant when determining the friction coefficient between the sliding surfaces in the presence of a fluid lubricant. Thus, the ability to vary these parameters must be considered when designing a novel tribometer to overcome the previously mentioned shortcomings of commercial drilling mud tribometers.

This article describes a novel, low-cost tribometer or lubricity tester designed specifically to address these issues and explore the influence of temperature, materials, lubricant, normal load, and sliding speed, as well as perform friction tests on drilling muds and sample materials (such as core samples) collected from a drilling site to compare laboratory-based measurements with those collected on site. The latter presents a significant issue, as often the friction testing results collected in the lab do not have the same performance during field testing and represent a significant hindrance to the development of new drilling muds for improved horizontal reaches in horizontal well drilling operations. First, the design of the tribometer will be outlined, including a description of the key components of the tribometer. Second, measurement of a steel-on-steel contact in deionized water will be acquired, such that performance of the tribometer can be compared with results obtained on a commercial tribometer. Finally, the performance of the tribometer with the addition of various lubricants for a steel-on-steel and steel-on-rock sliding configuration will be presented to demonstrate the instrument reaching its design specifications.

Design of the Tribometer

Fig. 1a shows a rendered image of computer-aided design model of the purpose-built tribometer. A direct current motor was used that could spin at variable speeds, controlled by a motor controller and a variable resistance potentiostat. The motor was able to spin in both clockwise and counterclockwise directions. The motor turned a drive shaft that mechanically couples into a torque sensor (4520A Torque Sensor, Kistler, Amherst, NY) that was able to measure the applied torque as well as the rotation speed. Digital readout of the torque sensor data was realized through a computer connected data acquisition system Data Acquisition (DAQ – National Instruments 6363, Austin, TX). All data taken in this article were acquired at 100 kHz without filtering the data. Post-processing of this data through a 20-point averaging routine reduced the effective sampling rate to 5 kHz. The torque sensor was mechanically connected to a "bob," or a steel cylinder, that was housed in the chamber constructed of 304 stainless steel (labeled in Fig. 1a), such that the rotation speed of the motor exactly matched that of the bob. For all experiments reported in this article, the bob was comprised of 4140 steel. A port at the bottom of the lubricant chamber allowed for facile emptying of the lubricant, which had a maximum volume of 1.2 L, from the chamber. Furthermore, the bob was designed such that it was user replaceable, allowing for surface treatments to the bob or replacement of a bob composed of varying materials. The cylindrical bob was 50 mm long and had a 25-mm diameter. The four posts surrounding the lubricant reservoir supported the weight platform and were machined from the same 304 stainless steel used in the construction of the lubricant reservoir. A cylindrical post in the center of the weight platform supported the addition of weights onto the platform, which allowed for control of the mechanical load transferred to the bob by the counter surface. A vice was placed under the weight platform, which allowed

FIG. 1 (a) Two-dimensional computer-aided design model of a cross section through the middle of the tribometer. Key components of the tribometer, including the weight platform (for varying the applied normal load), the chamber (storage of the lubricants tested), a torque sensor (for measuring the friction coefficient), a variable speed motor, drive shaft, the jaw couplers used to connect the drive shaft for the bob to the torque sensor and the variable speed motor, the samples relevant for the friction measurement (bob and counter surface), and the sliding interface have been labeled. The rotational movement of the bob/drive shaft has been labeled with a dotted line and labeled with the moment (τ) used to produce the rotational movement of the bob. (b) Photograph of the home-built tribometer after construction.

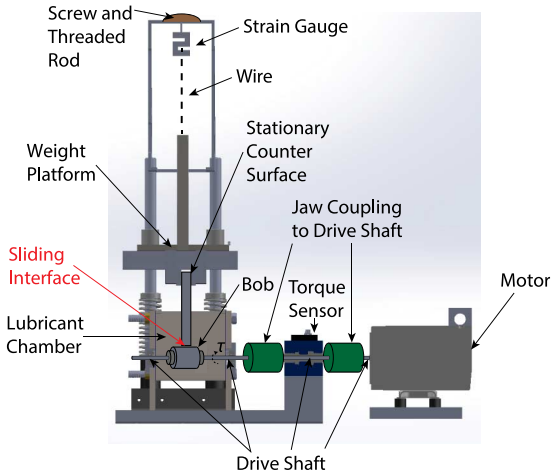

(a)

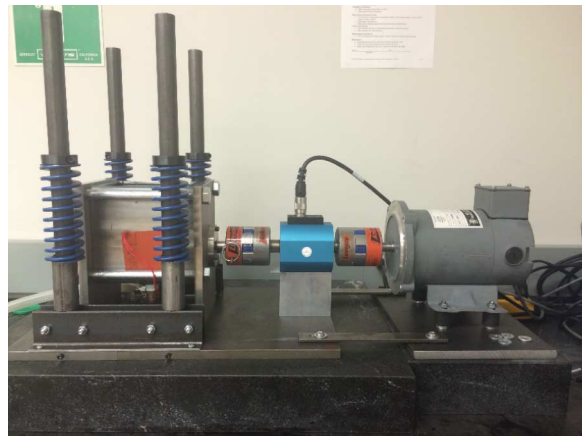

(b)

one to mechanically clamp the counter surface (i.e., core sample) to be tested, attaching it securely to the weight platform. For all experiments discussed in this article, this counter surface was either a rectangular 316 stainless steel block having dimensions of 18 by 64 by 100 mm^3 or a cylindrical sandstone core sample (Berea Sandstone Petroleum Core, 100–200 mD permeability, Cleveland Quarries, Vermilion, OH) having a diameter of 38 mm and a length of 115 mm. In all cases, the flat side of the counter surface, that being the rectangular steel block or the core sample, was held stationary and pressed against the rounded edge of the cylindrical bob, making a line contact between the two that resulted in a pure sliding motion when the bob was rotated. The mass of the weight platform was determined to be 12 kg. A support structure above the weight platform that could lift the weight platform was built, which included a load cell (Interface – Model SM100 – Interface, Scottsdale, AZ) and associated DAQ, such that the measured variance in the normal load could be recorded, as well as the reduction in load as the weight platform is lifted up during experiments. With this setup, the normal load applied to the bob by the counter surface could be varied from 20 N to 120 N by turning a lead screw/threaded rod that moved the weight platform vertically and the strain gauge measured the force in the wire attaching the load platform to the load cell. The actuation of the load platform from above allowed the counter surface to contact the bob at varying normal forces through the open face of the lubricant reservoir. The open top face of the lubricant reservoir allowed one to easily confirm the level of the lubricant, examine changes in the lubricant clarity or color during experimentation, and ensure that pressure was not built up in the lubricant reservoir during testing when the temperature of the lubricant bath was varied. Additionally, the load platform was allowed to move freely in the vertical direction,

supported through four bearings that fit snugly around the posts surrounding the lubricant reservoir. The free vertical movement of the load platform allowed for a constant applied normal force to the bob by the counter surface, which could decrease in length over the course of an experiment should significant wear result on the counter surface. Finally, the whole tribometer was placed on a granite block of 610 by 460 by 80 mm^3 dimensions, excluding the motor. To reduce the influence of mechanical vibrations from the motor on the friction measurements, the motor was isolated on its own granite block and placed on viton washers. Two guiding plates fixed the granite supports together to facilitate the alignment of the motor drivetrain with respect to the rest of the tribometer. **Fig. 1b** shows a photograph of the real setup that had been developed from **Fig. 1a**.

Determination of the friction force from this rotating bob and fixed counter surface was realized by measuring the torque the motor must exert on the bob to rotate it at a given speed. The torque on the bob was resolved using Eq 1:

$$F_f = \frac{\tau}{R} \tag{1}$$

where the F_f is the friction force, τ is the measured torque from the torque sensor, and R is the radius of the rotating bob. In this configuration, the counter surface is held stationary and the bob is rotating about the shaft, coupled to the torque sensor and driving motor. The weight platform and associated counter surface was mounted such that the load was applied normal to the bob, and thus the applied normal force was calculated as the mass of the weight platform times the acceleration caused by gravity, minus the upward force on the weight platform exerted by the load cell. The friction coefficient was then calculated by dividing the friction force measured by the torque sensor by the applied normal force by the weight platform to the bob. Typical measurements were conducted for approximately 10 minutes, and then the acquired data were averaged using a weighted average of the nearest 20 data points. These averaged data were then used to determine the average friction coefficient. Before every friction experiment, the torque required to turn the bob and supporting shaft without any load applied (i.e., the weight platform and associated counter surface were removed), and thus measured by the torque sensor, was acquired for 1 minute at the desired revolutions per minute of the experiment. The average value of the torque measured during this time was then subtracted from subsequent values of the torque measured once the load was applied during the experiment. In all experiments reported in this article, we assume that additional friction resulting from the increased load on the bearings that support the bob is negligible in relation to the high friction of the sliding contact of the bob and the counter surface. The variation in the measured friction coefficient with sliding speed and applied load is reported in terms of the sliding speed in revolutions per minute of the bob divided by the applied load, as these are the parameters that users typically report in the drilling.

Calibration of Tribometer

Before measuring the performance of a drilling mud and associated lubrication additives in the tribometer, the coefficient of friction for the steel counter surface sliding against the steel bob in deionized water was measured. In commercial testing manuals, steel-on-steel friction coefficient measured in the presence of deionized water as a lubricant at a value of 0.34 ± 0.05 must be confirmed as a method to identify the correct operation and alignment

FIG. 2 (a) Friction coefficient versus time for a steel-steel contact lubricated by deionized water under 120 N normal load and 60 r/min rotational speed. The average friction coefficient measured between 50 and 300 seconds was determined to be 0.34 ± 0.02. (b) Friction coefficient versus inverse load for a steel-steel contact lubricated in deionized water. The load was varied from 20–120 N in the experiments shown in (b). Error bars represent the standard deviation in the mean values taken from comparable graphs to (a) from time ranging from 50 to 300 seconds.

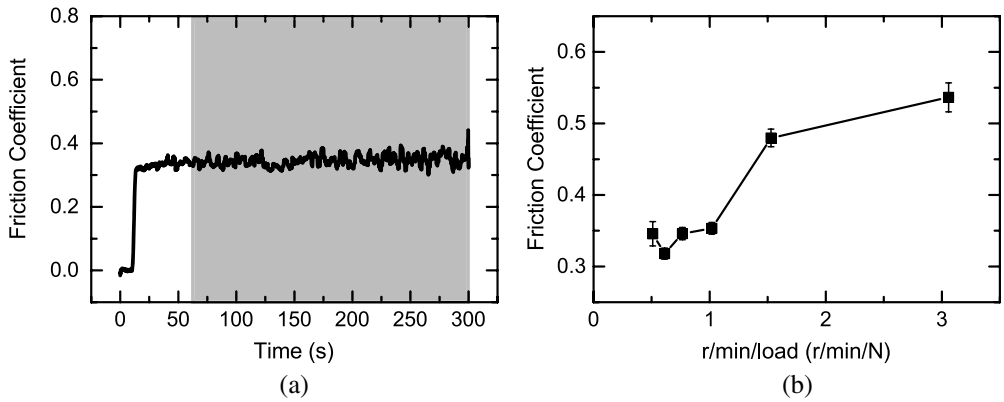

of the various components of the commercial machine [6]. This procedure is often referred to as calibration, as it provides a value of a friction coefficient against which subsequent measurements can be standardized. For these tests, the bob was rotated at 60 r/min, the load was 120 N (no weight taken off the weight platform by the load cell), and the temperature was not controlled but was ~21°C at the onset of testing. Fig. 2a shows an example friction coefficient versus time measurement taken under these conditions. Initially, the average torque value was measured for approximately 10 seconds at 60 r/min while no weight was pressed against the bob. This allowed for the determination of the force required to spin the bob in the lubricant. Subsequently, the counter surface and the associated weight were added, and the bob rotation speed was adjusted to maintain the 60 r/min rotational speed. No data were recorded during the time that it takes to add the weight and adjust the rotational speed of the bob, and therefore no data are visible for that time in Fig. 2a or subsequent graphs showing friction coefficient versus time. Additionally, most run-in behaviour was completed while the rotational speed of the bob was adjusted and was therefore not recorded in the displayed data sets collected in the subsequent figures. All calibration measurements were made for 5 minutes at 60 r/min, which is the calibration procedure specified in Ref. [6]. An average friction coefficient was determined by averaging all measured values of the friction coefficient from time 50 seconds, or once the friction coefficient reached a steady-state value, until the end of the measurement time period. The associated standard deviation in this mean value was also determined and given as the error in the measured average friction coefficient.

The friction coefficient for this steel-steel contact was determined to be 0.34 ± 0.02 in Fig. 2a for deionized water, comparable to that required in the calibration of comparable existing tribometers [6]. Thus, the same calibration value was required whenever the tribometer was tested under these conditions. In instances when the friction coefficient was significantly off from this value, remachining or sanding the bob/steel counter surface corrected the issue. A higher degree of variance, quantified in terms of a larger standard deviation, was observed in the friction coefficient versus time when the counter surface was

not aligned properly, such that the bob and counter surfaces did not make intimate contact (i.e., the counter surface was tilted with respect to the surface of the bob). Finally, before each calibration measurement, the lubricant reservoir, counter surface, and bob were cleaned first with acetone and subsequently ethanol to remove any organic contaminants, wear particles, or other debris from the sliding interface or chamber itself.

Similar measurements of the friction coefficient versus time were acquired at 60 r/min rotational speed and with deionized water present in the lubricant chamber while varying the applied load between 20–120 N in increments of 20 N. **Fig. 2b** shows the result of this type of measurement, where the friction coefficient was plotted against rotational speed divided by load in the effort to begin construction of a Stribeck curve. A Stribeck curve can be used to identify the mechanism of lubrication and thus the function of the lubricant used in a given application for a given set of engineering parameters or operating conditions, such as contact stresses, sliding speeds, and fluid viscosity [9]. For example, under high loads and slow sliding speeds, the lubricating fluid must reduce the surface energy and adhesion of the sliding surface, as they are in direct contact. These conditions are referred to as boundary lubricating conditions. At low loads and high sliding speeds, a fluid lubricant can push the two solid surfaces apart and significantly reduce friction by preventing direct contact of any part of the solid materials. In this lubrication regime, called hydrodynamic lubrication, the viscosity and drag induced by the flowing lubricant can be the critical parameter to control in designing a lubricant. Generating a Stribeck curve allows one to identify the mechanism of lubrication and custom tailor the lubricant with greater precision for the application. While **Fig. 2b** does not show the influence of the lubricant viscosity, nor does the x axis show the Hersey number, as is typical of Stribeck curves, what is shown is the variation of the friction coefficient with rotational speed measured and the applied load, which are two of the parameters that are varied when constructing a Stribeck curve. Furthermore, resulting from the limitations of the design of the experimental apparatus, primarily in the low loads that could be detected and limitations on the maximum rotational speed that could be achieved, a complete Stribeck curve showing changes in the lubrication regimes could not be acquired. However, **Fig. 2b** showed no variation in the friction coefficient was observed for the larger load (60–120 N) ranges investigated. However, a significant increase in the friction coefficient was observed for lighter loads (20 and 40 N applied loads). Assuming Hertzian contact mechanics for a flat-on-cylinder geometry, the maximum pressure applied between the surfaces can be determined using the following formula [10]:

$$P_{max} = \left(\frac{E^* N}{\pi L R}\right)^{\frac{1}{2}} \tag{2}$$

where P_{max} is the maximum contact pressure, E^* is the reduced elastic modulus (or the elastic modulus of steel for a steel-on-steel contact), N is the vertical force applied to the bob by the weight platform, L is the length of the contact, and R is the radius of the bob. The vertical force applied to the bob by the weight platform corresponds to the mass of the weight platform times the acceleration due to gravity minus the upward force exerted by the load cell on the load platform. The maximum pressures applied ranged from 43 MPa to 105 MPa for loads of 20–120 N loads used, assuming an elastic modulus for steel of 200 GPa [11]. These stresses are well below the yield stress, which is approximately 200 MPa for steel [11], meaning that elastic deformation of the bob and counter surface was expected in the load ranges studied. This load range also replicated the contact

pressures reported for similar studies of drill lubricants, which were on the order of 30 MPa [12] to 140 MPa [13]. Given the relatively large stresses and the low viscosity of water in comparison with oil, Fig. 2b indicates that boundary lubricant was the most likely lubrication regime and that a fluid film has not developed between the bob and the counter surface. However, a significant increase in sliding speed and load would be required to verify the exact mechanism of lubrication, as a clear transition between boundary lubrication and elastohydrodynamic lubrication was not observed for the load ranges investigated.

Lubricant Additive Measurements

Four commercially available lubricant additives used in the industry were tested to observe their influence on the friction coefficients. These lubricants were proprietary lubricant additives used in industry and labeled Additive 1 through 4. Lubricant additives were dispersed in deionized water at a concentration of 1 %, 3 %, and 5 % by volume. Fig. 3a shows the variation in the performance of the lubricant at reducing the friction coefficient measured versus time for a 120 N applied load, a rotational speed of 60 r/min, and a concentration of 3 %. Under these conditions, Additive 3 performed the best compared

FIG. 3 (a) Measured friction coefficient versus time for Additives 1–4 at 3 % concentration, load of 120 N, and rotation speed of 60 r/min. (b) Stribeck curve for the four lubricant additives at 60 r/min and 3 % concentration. (c) The variation in the Stribeck curve for Additive 3 at 60 r/min for 1 %, 3 %, and 5 % concentrations of the additive. (d) Stribeck curve for 1 % of Additive 3 at varying rotational speeds of the bob. Error bars represent the standard deviation in the mean values of the friction coefficient.

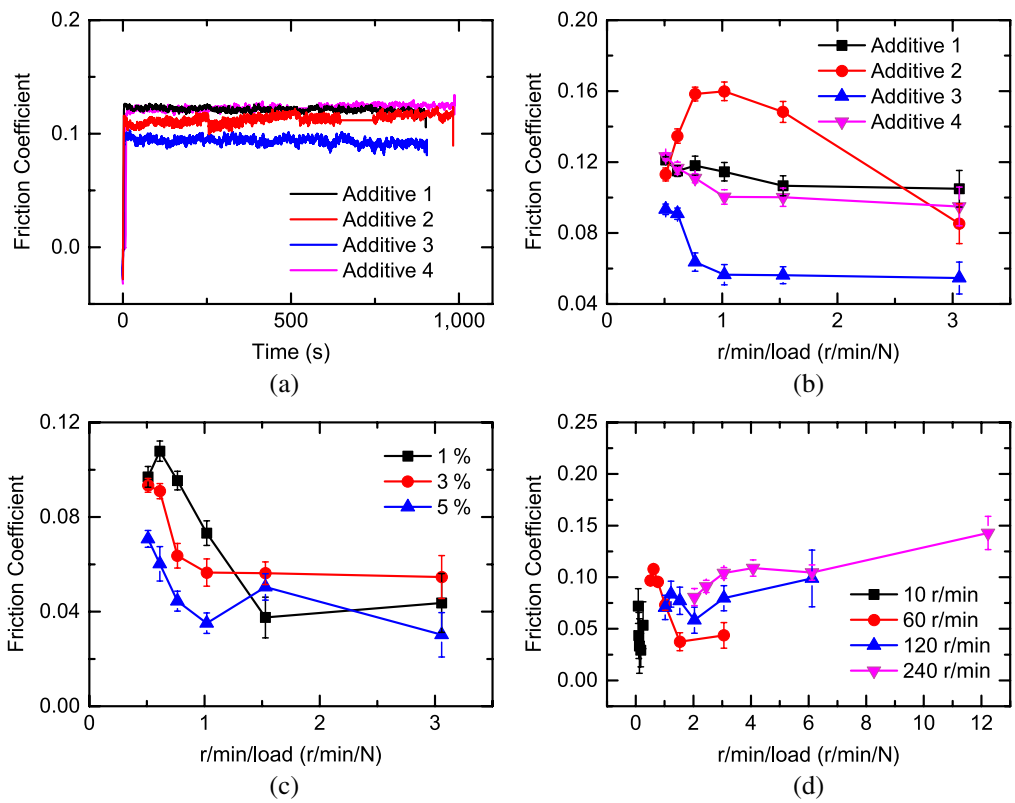

with the other lubricant additives. Fig. 3b shows a Stribeck curve for the four lubricant additives at 3 % concentration. Additionally, the load-dependent behavior of the four additives varied significantly. A Stribeck curve was generated for Additive 3 at various concentrations of the additive, as shown in Fig. 3c. Here, it is possible to see that an increase in the concentration of the additive had a significant influence on the ability of the lubricant to reduce friction in a steel-steel sliding contact, particularly at higher loads. At lower loads (20–40 N), an increase in the concentration of the lubricant additive did not have a significant influence on the measured friction coefficient. Fig. 3c shows an extended Stribeck curve for Additive 3 at a concentration of 1 %. This curve was developed by varying the load from 20–120 N for a given speed of 10, 60, 120, and 240 r/min. Although an exact overlap between the various measurements at difference speeds was not observed, a general trend of increasing friction coefficient with increasing revolutions per minute and inverse applied force is observed for Additive 3 at 1 % concentration in deionized water.

Steel-on-Core Sample Friction Testing

Fig. 4a shows the friction coefficient versus time for a sandstone core sample sliding against the steel bob in deionized water and a 3 % concentration solution of Additive 4 with a 40 N load applied to the bob. The friction coefficient for deionized water lubrication was 0.55 ± 0.05 and for Additive 4 at 3 % concentration the friction coefficient was 0.24 ± 0.01. In comparison to the steel-on-steel contact, the friction coefficient for the sandstone-on-steel contact was much higher. Additionally, a significantly greater variation in the friction coefficient was observed, quantified through the standard deviation in the mean friction coefficient. This greater variation was likely a result of the higher roughness of the sandstone core sample compared with the machined finish of the steel sample. Fig. 4b shows a Stribeck curve for the core sample sliding against the steel bob lubricated by deionized water and at 3 % Additive 4 conditions. The trends observed in Fig. 4b do not show the same variance with r/min/load that was observed in Fig. 3b. This variance was a result of the increased roughness of the sandstone rock, in comparison to the machined steel surface, in combination with the thickness of the fluid film that was likely present between the two surfaces. However, an exact determination of this would

FIG. 4 (a) Friction coefficient versus time for the sandstone core sample sliding against the steel bob in deionized water (black) and Additive 4 at 3 % concentration (red) and 40 N load. (b) Stribeck curve for the sandstone core sample in water and the same Additive 4 at 3 % concentration.

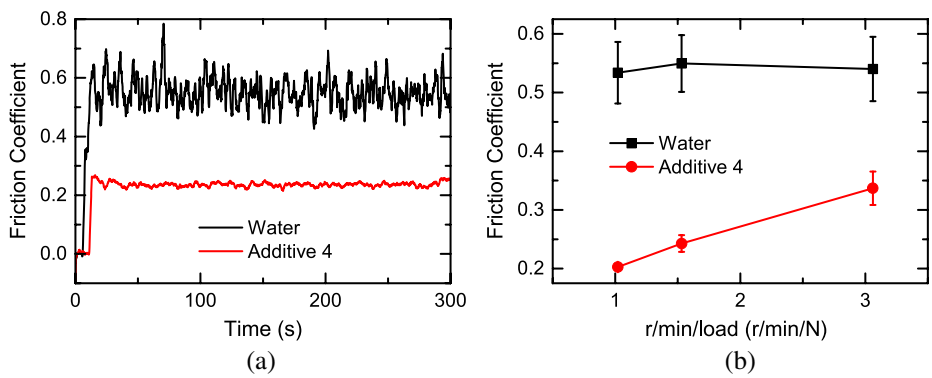

require a much greater variation in the sliding speeds and loads than was achieved in this study. The smaller range of r/min/load used in **Fig. 4b** compared with those used for the steel-on-steel contacts in **Fig. 3** was a result of the decreased mechanical properties in terms of yield strength of the core sample compared with the machined steel counter surface. One implication of this was that a significant amount of wear particles from the sandstone-on-steel pair was generated in the lubricant during friction testing compared with the same test conditions conducted on the steel-on-steel contacting pair, resulting in the lubricant becoming opaque by the end of the friction test. In the steel-on-steel friction tests, no wear particles were observed in the lubricant bath upon visual inspection of the lubricant after friction testing.

Conclusions and Outlook

A new tribometer for the evaluation of drilling muds was developed. The tribometer was specifically designed to allow for sliding tests for materials relevant for horizontal well drilling operations, specifically steel-on-steel contacts and steel-on-rock contacts. The lubricating properties of various proprietary friction-reducing additives were observed when used in water-based drilling muds showing that in the friction coefficients measured under varying load and speed conditions. A significantly higher friction coefficient under the test conditions comparable to those used by the commercially available lubricity meters (60 r/min, 120 N load, room temperature) with deionized water lubrication was observed for a steel-on-sandstone contact (0.55 ± 0.05) compared with a steel-on-steel contact (0.34 ± 0.02). In all cases, the addition of the friction-reducing additives to the deionized water resulted in a lower friction coefficient for both the steel-on-steel and steel-on-sandstone measurements. Finally, while a conclusive statement of the lubrication regime cannot be made at this time under the conditions friction measurements were made, the high pressures applied to the sliding interface and the low viscosity of the lubricants suggest that the likely lubrication regime was in the boundary regime. Improvements to the tribometer to increase the range of speeds attainable, as well as the range of loads that can be tested, will be critical to determining the lubrication mechanism with greater precision. Furthermore, continued development of such tribometers will be critical for real improvements in drilling muds, as the demonstrated difference in friction coefficients measured between steel-on-steel contacts and steel-on-sandstone contacts are significant.

ACKNOWLEDGMENTS

The authors would like to acknowledge funding for this project through the Natural Sciences and Engineering Research Council (NSERC) Engage Grants. The authors would like to also thank Matt DeWit and Eric Sonmor at Secure Energy Services for their support of the project.

References

[1] Mirhaj, S. A., Fazaelizadeh, M., Kaarstad, E., and Aadnoy, B. S., "New Aspects of Torque-and-Drag Modeling in Extended-Reach Wells," presented at the *SPE Annual Technical Conference and Exhibition*, Florence, Italy, Sept. 20–22, 2010, Society of Petroleum Engineers, Richardson, TX, 13p.

[2] Aadnoy, B. S., Stavanger, U., and Andersen, K., "Friction Analysis for Long-Reach Wells," presented at the *IADC/SPE Drilling Conference*, Dallas, TX, March 3–6, 1998, Society of Petroleum Engineers, Richardson, TX, pp. 819–834.
[3] Apaleke, A. S., Al-Majed, A. A., and Hossain, M. E., "Drilling Fluid: State of The Art and Future Trend," presented at the *North Africa Technical Conference and Exhibition*, Cairo, Egypt, Feb. 20–22, 2012, Society of Petroleum Engineers, Richardson, TX, pp. 20–22.
[4] Dobson, J. W., Harrison, J. C., Hale, A. H., Lau, H. C., Bernardi, L. A., Jr., Kielty, J. M., Albrecht, M. S., and Bruner, S. D., "Laboratory Development and Field Application of a Novel Water-Based Drill-In Fluid for Geopressured Horizontal Wells," *SPE Drill. Complet.*, Vol. 15, No. 2, 2000, pp. 105–111, https://doi.org/10.2118/64112-PA
[5] Growcock, F. B., Frederick, T. P., Reece, A. R., Green, G. W., and Ruffin, M. D., "Novel Lubricants for Water-Based Drilling Fluids," presented at the *SPE International Symposium on Oilfield Chemistry*, Houston, TX, Feb. 16–19, 1999, Society of Petroleum Engineers, Richardson, TX, 11p.
[6] "Extreme Pressure and Lubricity Tester Instruction Manual," OFI Testing Equipment, Houston, TX, 2015, pp. 1–26.
[7] Erdemir, A., "Review of Engineered Tribological Interfaces for Improved Boundary Lubrication," *Tribol. Int.*, Vol. 38, No. 3, 2005, pp. 249–256, https://doi.org/10.1016/j.triboint.2004.08.008
[8] Spikes, H. and Jie, Z., "History, Origins and Prediction of Elastohydrodynamic Friction," *Tribol. Lett.*, Vol. 56, No. 1, 2014, pp. 1–25, https://doi.org/10.1007/s11249-014-0396-y
[9] Bowden, F. P. and Tabor, D., "Friction and Surface Damage of Sliding Metals," *The Friction and Lubrication of Solids*, Oxford University Press, Oxford, United Kingdom, 1986, pp. 73–89.
[10] Johnson, K., *Contact Mechanics*, Reprint ed., Cambridge University Press, Cambridge, United Kingdom, 1987, 468p.
[11] Callister, W. D. and Rethwisch, D. G., *Materials Science and Engineering: An Introduction*, 9th ed., John Wiley and Sons, Hoboken, NJ, 2014, 960p.
[12] Al-Mehailan, M. S., Al-Foudari, S. J., Debroy, A., Rajagopalan, A., Abou Elkhair, M., and McNaughton, P., "Novel Lubricant—Bridging Agent Combination Cures Differential Sticking Problems in High Pressured North Kuwait Wells," presented at the *IADC/SPE Asia Pacific Drilling Technology Conference*, Bangkok, Thailand, Aug. 25–27, 2014, Society of Petroleum Engineers, Richardson, TX, 12p.
[13] Bol, G. M., "Effect of Mud Composition on Wear and Friction of Casing and Tool Joints," *SPE Drill. Eng.*, Vol. 1, No. 5, 1986, 8p.